Synthesis, Characterization, and Properties of Silicone–Epoxy Resins

Xin Yang,[1,2] Wei Huang,[1] Yunzhao Yu[1]

[1]*Institute of Chemistry, Chinese Academy of Sciences, Beijing 10080, People's Republic of China*
[2]*Graduate University of Chinese Academy of Sciences, Beijing 10039, People's Republic of China*

Received 27 April 2010; accepted 27 July 2010
DOI 10.1002/app.33108
Published online 9 November 2010 in Wiley Online Library (wileyonlinelibrary.com).

ABSTRACT: Silicone–epoxy (SiE) resins were synthesized through the hydrolytic condensation of 2-(3,4-epoxycyclohexylethyl) methyldiethoxysilane (EMDS) and the cohydrolytic condensation of EMDS with dimethyldiethoxysilane. Structural characterization was carried out by ^{1}H-NMR, ^{29}Si-NMR, and mass spectrometry analysis; the resins were linear oligomers bearing different numbers of pendant epoxy groups, and the average number of repeat Si—O units ranged from 6 to 11. Methyhexahydrophthalic anhydride was used to cure the SiE resins to give glassy materials with high optical clarity. The cured SiE resins showed better thermal stability and higher thermal and UV resistances than a commercial light-emitting diode package material (an epoxy resin named CEL-2021P). The effect of the epoxy value on the thermal and mechanical properties and the thermal and UV aging performances of the cured SiE resins were investigated. The SiE resins became more flexible with decreasing epoxy value, and the resin with the moderate epoxy value had the highest thermal and UV resistances. © 2010 Wiley Periodicals, Inc. J Appl Polym Sci 120: 1216–1224, 2011

Key words: silicone-epoxy resin; hydrolytic condensation; thermal and UV resistance; light-emitting diodes (LED) package

INTRODUCTION

Solid-state lighting technology based on high-brightness white light-emitting diodes (LEDs) promises a reduction in power consumption compared to that of conventional lamps. Generally, white light is obtained by the excitation of a phosphor with short-wavelength light emitted by GaN-based chips. High brightness means high light output intensity, and subsequently, LED devices have to undergo a high intensity of UV light and a high working temperature; these accelerate the aging of the encapsulation materials. Currently, most LEDs are packaged with epoxy resins. Normal epoxy resins, such as bisphenol A epoxy resins, undergo thermal and UV aging and display very pronounced yellowing or discoloration with long-time exposure to light and heat; these seriously decrease their luminous efficiency.[1,2] The improvement of the thermal and light aging resistances of LED encapsulation materials is a very important issue.

Silicone–epoxy (SiE) resins, which combine both the advantages of epoxy resins and silicone resins, are promising as ideal materials for LED encapsulation.[3–10] On the one hand, they are less sensitive than epoxy resins to heat and UV light because of the high bond energy of Si—O; on the other hand, they can overcome the poor adhesive and mechanical properties of silicone resins. SiE resins with optimum thermal and mechanical properties can be obtained by the introduction of different proportions of the siloxane component through hydrosilylation[11,12] or a hydrolytic condensation process.[13–16]

In this study, novel SiE resins were synthesized by the base-catalyzed hydrolytic condensation of 2-(3, 4-epoxycyclohexylethyl) methyldiethoxysilane (EMDS) and by the cohydrolytic condensation of EMDS with dimethyldiethoxysilane. Our aims were to determine the advantages of SiE resins over normal epoxy resins and to examine the effect of the epoxy group content on the properties of the SiE resins.

EXPERIMENTAL

Materials

Methyldiethoxysilane and dimethyldiethoxysilane were purchased from Jilin Huafeng Organosilicon Co., Ltd. (China), and 1,2-epoxy-4-vinylcyclohexane was purchased from Synasia (SuZhou) Co., Ltd. (China). These compounds were purified by vacuum distillation before use. The Karstedt catalyst (a platinum–divinyltetramethyldisiloxane complex) was obtained from Degussa (Evonik Degussa Co., Ltd., China) and was used as received. Methyhexahydrophthalic anhydride (MeHHPA) and the curing accelerator tetra-*n*-butylphosphonium *o*,*o*′-diethylphosphotodithioate (PX-4ET) were supplied by Polynt S.p.A., (Italy) and Nippon Chemical Industrial Co.,

Correspondence to: W. Huang (huangwei@iccas.ac.cn).
Contract grant sponsor: National High-Tech R&D Program of China (863 program); contract grant number: 2006AA03A136.

LTD. (Japan), respectively. 3,4-Epoxycyclohexylmethyl-3,4-epoxycyclohexane carboxylate (CEL-2021P, epoxy value 0.74) was a commercially available epoxy resin for LED encapsulation and was supplied by Daicel Chemical Industries, Ltd. (Japan).

Synthesis

Synthesis of EMDS

Methyldiethoxysilane (40.2 g, 0.5 mol) was loaded into a 250-mL, three-necked, round-bottom flask equipped with a thermometer, a reflux condenser, and a magnetic stirrer. A 1% Karstedt catalyst–isopropyl alcohol solution (0.41 g) was added to the flask, and then, the reaction mixture was heated to 80°C. 1,2-Epoxy-4-vinylcyclohexane (40.92 g, 0.33 mol) was added dropwise in 1 h via a dropping funnel, and the reaction was continued for a further 30 min to give the crude product, which was purified by vacuum distillation, and the fraction at 104°C/1 mmHg was collected as the product EMDS.

Synthesis of the SiE resin SiE-1

EMDS (20.64 g, 0.08 mol), deionized water (2.88 g, 0.16 mol), and NaOH (0.04 g) were added to a 100-mL, three-necked, round-bottom flask equipped with a reflux condenser, a thermometer, and a mechanical stirrer. The reaction mixture was stirred at 20°C for 12 h. The ethanol generated in the reaction was distilled off, and 60 mL of toluene was added. The solution was then washed with deionized water several times until it reached a pH of 7. Then, *n*-hexane was added to the toluene solution, and the precipitated material was collected. The residual solvent was evaporated under reduced pressure to give the product SiE-1, a colorless viscous liquid.

Synthesis of the SiE resins SiE-2 and SiE-3

EMDS (10.32 g, 0.04 mol), dimethyldiethoxysilane (2.96 g, 0.02 mol), deionized water (2.16 g, 0.06 mol), and NaOH (0.03 g) were loaded into a 100-mL, three-necked, round-bottom flask equipped with a reflux condenser, a thermometer, and a mechanical stirrer. The reaction mixture was stirred at 20°C for 6.5 h. Next, the ethanol generated in the reaction was distilled off, and 30 mL of toluene was added. The solution was then washed with deionized water several times to neutral pH. Then, the solvent was distilled off under reduced pressure to give the product SiE-2, a colorless viscous liquid. SiE-3 was synthesized by the same procedure, except the molar ratio of EMDS to dimethyldiethoxysilane was 1:1.

Curing procedures and aging tests

SiE-1, SiE-2, SiE-3, and CEL-2021P were mixed with MeHHPA, respectively, according to the stoichiometry; the mass ratio of the accelerator PX-4ET to MeHHPA was 1:50. The mixtures were degassed *in vacuo* and then poured into 2 mm thick molds.[17] The curing was conducted at 120°C for 2 h and then at 150°C for 1 h. The samples were removed from the molds after they were cooled to room temperature. Thermal aging was performed at 150°C in a circulating air oven, and UV aging was accomplished in a UV aging oven. The wavelength of the UV light was 310 nm, and the radiation intensity of the resin surface was 300 mW/cm^2.

Measurements

^{1}H-NMR and ^{29}Si-NMR spectra in $CDCl_3$ were recorded on a Bruker Avance400 MHz NMR spectrometry at room temperature. The viscosities of the SiE resins were measured on a Brookfield model DV-II+ cone and plate viscometer (Brookfield Co., USA). Mass spectrometry (MS) analysis was performed on a Bruker Biflex III matrix-assisted laser desorption/ionization (MALDI-TOF)–MS spectrometer. The surface atomic compositions of the cured SiE resins were analyzed by an ESCALab220i-XL X-ray photoelectron spectrometer (VG Scientific, UK) with a 300-W Al Kα X-ray source; the base pressure was about 3×10^{-9} mbar, and the sample was analyzed at a takeoff angle of 15°. Transmittance spectra of the SiE resins (placed in a 10 mm thick quartz

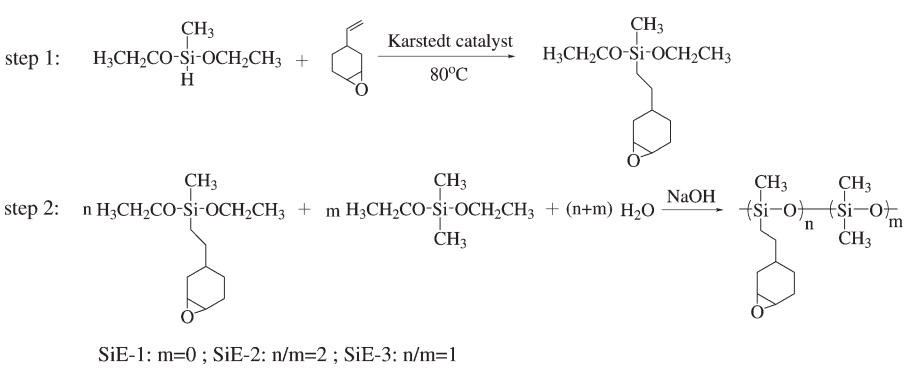

Scheme 1

TABLE I
Synthesized SiE Resins

Sample	*m:n*	$m + n$[a]	Silicon content (%)	Viscosity (cp)	Epoxy value[b]
SiE-1	0	8–9	15	18,000	0.503
SiE-2	1:2	6–7	19	1,280	0.407
SiE-3	1:1	10–11	23	650	0.356

[a] Estimated from the ^{1}Si-NMR spectra. m denotes the number of 2-(3,4-epoxycyclohexylethyl) methyl siloxane units and n denotes the number of dimethyl siloxane units.
[b] Measured with a hydrochloride–butanone titration method.

absorption cell) and the cured samples were measured on a Unico UV-4802 UV-vis spectrophotometer (Unico Instrument Co., Ltd., Shanghai) in the range 300–800 nm, and the yellowness index (YI) were calculated from the spectrum intensity. Differential scanning calorimetry (DSC) was performed on a SII EXSTAR6000-DSC6220 (Seiko, Japan), and thermogravimetric analysis (TGA) was carried out on an SII EXSTAR6000-TGA6300 in nitrogen at a heating rate of 10°C/min. Dynamic mechanical analysis (DMA) was carried out on a TA Q800 (TA Instruments, New Castle, USA) in the double-cantilever mode under a nitrogen atmosphere at a frequency of 1 Hz and at a heating rate of 5°C/min. Thermomechanical analysis (TMA) was performed on a TA Q400 at a heating rate of 5°C/min under a flow of N_2 gas. The hardness of the cured samples was measured with a LX-D Shore D Durometer (Haibao Instrument Co., Ltd., China) according to ASTM D 2240.

RESULTS AND DISCUSSION

Synthesis and characterization of SiE resins

SiE resins can be synthesized by hydrosilylation between a polysiloxane containing Si—H bonds and an epoxide containing vinyl groups.[7,18] However, the catalysts most used for hydrosilylation, such as platinum or rhodium, are very difficult to separate, and residues of which will lead to a remarkable reduction in the transmittance of synthesized SiE resins. In this study, SiE resins were prepared by the hydrolytic condensation of silicon alkoxides (Scheme 1). Although the reagent used for the hydrolytic condensation, EMDS, was synthesized through platinum-catalyzed hydrosilylation, it was purified by distillation; thus, the platinum catalyst was removed easily.

Here, we used diethoxysilane rather than trimethoxysilane, such as 2-(3,4-epoxycyclohexylethyl)-trimethoxysilane, which is commonly used to prepare SiE resins in the literature for two reasons. First, the hydrolytic condensation of ethoxysilane is more controllable because it is less reactive than methoxysilane; second, the condensation of dialkoxysilane can only generate linear polysiloxanes, but gelation, which occurs easily in the condensation of trialkoxysilane, can be avoided.

Generally, the hydrolytic condensation of silicon alkoxides can be catalyzed by a proton acid or base. However, a proton acid catalyst was not suitable for this study because the epoxy groups would have undergone a ring-opening reaction with it. We chose sodium hydroxide as a catalyst and synthesized three SiE oligomers with different epoxy group contents by changing the molar ratio of EMDS to dimethyldiethoxysilane (Table I).

The ^{1}H-NMR, ^{29}Si-NMR, and MALDI-TOF spectra for SiE-1 are shown in Figures 1–3, respectively. We can see from the ^{29}Si-NMR and ^{1}H-NMR spectra that except for a very small amount of cyclic siloxanes (peak shift at −22.4 ppm in Fig. 2), SiE-1 was a linear polysiloxane with Si—OH end groups, and the

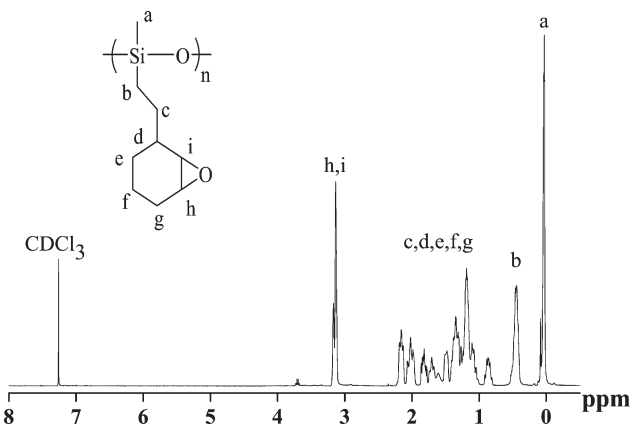

Figure 1 ^{1}H-NMR spectrum of SiE-1.

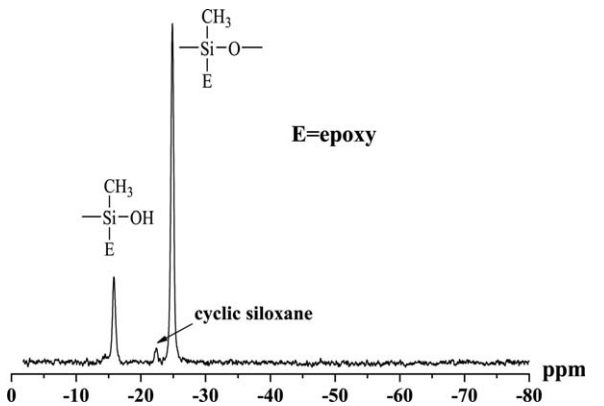

Figure 2 ^{29}Si-NMR spectrum of SiE-1.

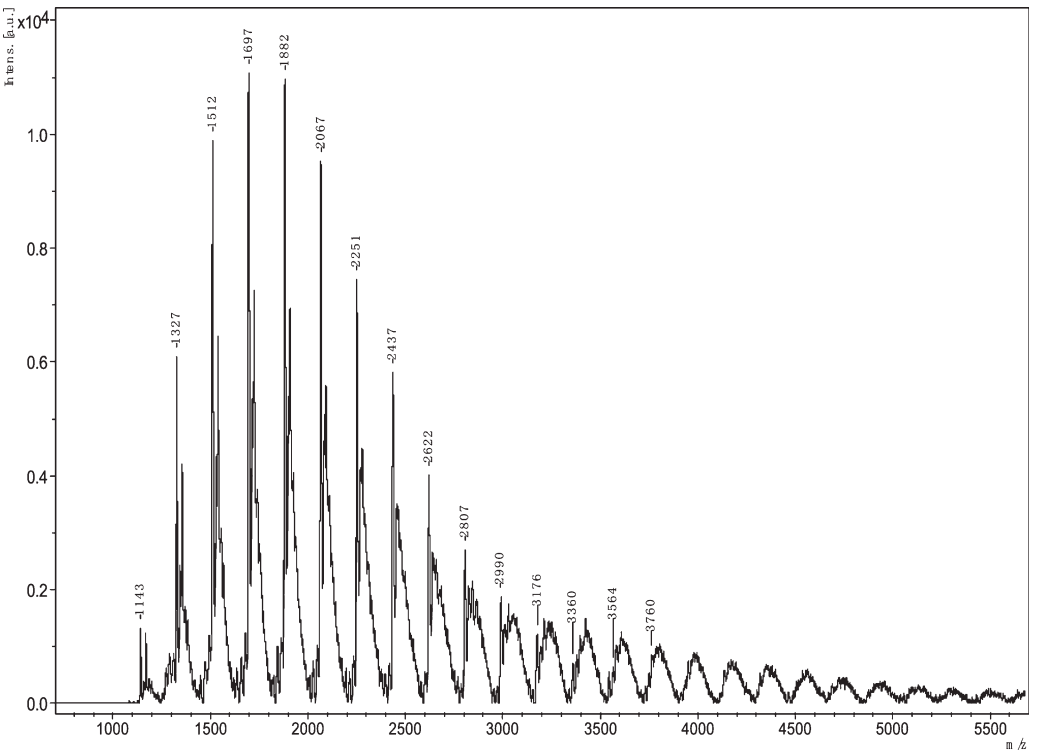

Figure 3 MALDI-TOF spectrum of SiE-1.

ethoxy groups almost disappeared after condensation. The number of repeat Si—O units of SiE-1, estimated from the ^{29}Si-NMR spectra, was 8–9; this means that the average molecular weight of SiE-1 was about 1800. This was confirmed by the MALDI-TOF results shown in Figure 3.

The SiE resins SiE-2 and SiE-3 had similar structures to that of SiE-1. As —$Si(CH_3)_2O$— segments were introduced, the relative content of epoxy groups decreased. The epoxy values of the silicone epoxy resin were measured through a hydrochloride–butanone titration method, and the results are listed in Table I. The viscosity of the SiE resin decreased with decreasing epoxy value, as shown in Table I, and the convenient adjustment of viscosity would make SiE resins useful for LED packaging.

A high optical transparency is important premise for use in LED encapsulation materials. SiE-1 was a highly transparent and colorless liquid, as clear as water, and its transmittance spectrum over the range from 300 to 800 nm is shown Figure 4. SiE-2 and SiE-3 were also very transparent, with transmittances over 90% at 400 nm.

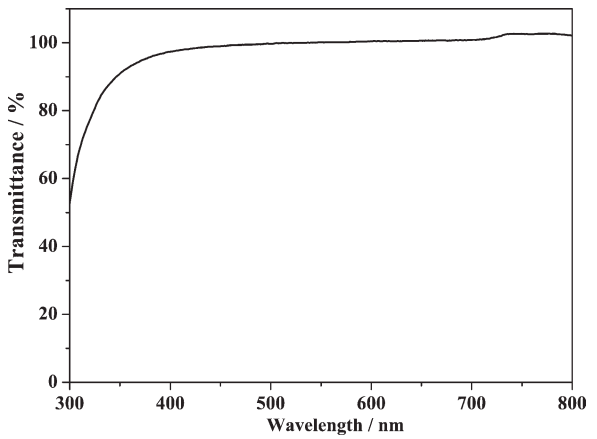

Figure 4 Transmittance spectrum of SiE-1.

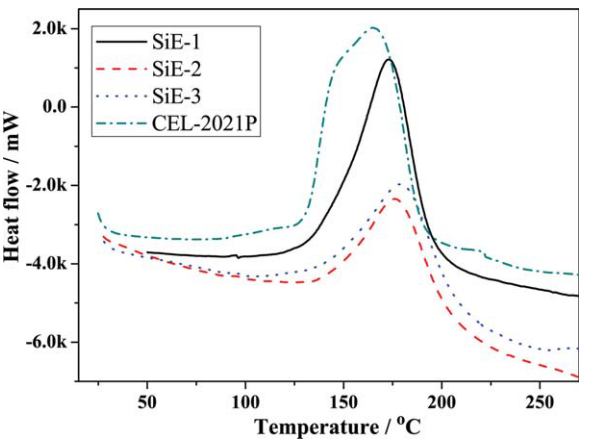

Figure 5 DSC curves of the SiE resin/MeHHPA and CEL-2021P/MeHHPA systems. [Color figure can be viewed in the online issue, which is available at wileyonlinelibrary.com.]

TABLE II
DSC and TGA Characteristics of the SiE Resin/MeHHPA and CEL-2021P/MeHHPA Systems

Sample	T_p (°C)	ΔH (mJ/mg)	$T_{5\%}$ (°C)	T_f (°C)	T_s (°C)
SiE-1	173	321	328.2	339.5	459.3
SiE-2	176	276	341.8	353.7	464.9
SiE-3	179	273	335.3	351.6	465.6
CEL-2021P	165	359	312.9	330.7	None

Curing of the SiE resins

MeHHPA is a commonly used curing agent for epoxy resins when they are used for LED encapsulation because MeHHPA-cured epoxy resins have several advantages, such as a high optical clarity and a high weather resistance. Figure 5 shows the DSC thermograms for the SiE resin/MeHHPA systems, with the CEL-2021P/MeHHPA system shown for comparison. The exothermic peak temperatures (T_p's) and exothermic enthalpies of the curing reaction (ΔH's) are summarized in Table II. All of the SiE resins showed a higher T_p than did CEL-2021P, the order of T_p for the SiE resins was as follows: SiE-3 > SiE-2 > SiE-1; this was consistent with the order of their epoxy values. Because the epoxy value of CEL-2021P was 0.74, which was higher than those of the SiE resins, the curing reactivities of the SiE resins were comparable to that of CEL-2021P. This was reasonable because their epoxy groups had very similar structures. Also, ΔH decreased with decreasing epoxy value.

The MeHHPA-cured SiE resins were glassy materials with a high transparency without any yellowing. Figure 6 shows the transmittance spectra in the range from 300 to 800 nm for the cured SiE resins and CEL-2021P; all four resins showed a high transmittance. However, at wavelengths below 450 nm, CEL-2021P showed an apparently lower transmittance compared to the SiE resins; this explained why the cured CEL-2021P exhibited slightly visible yellowing.

Thermal stability of the cured resins

Figure 7 gives the TGA curves for the MeHHPA-cured resins. A two-stage weight loss was observed for all of the cured SiE resins. The first weight loss occurred at about 340°C; this was close to the thermal decomposition temperature of the MeHHPA-cured CEL-2021P and was attributed to the decomposition of organic parts from anhydride and epoxy groups; the second weight loss occurred at about 450°C. This corresponded to the decomposition of siloxane chains. The values of the onset decomposition temperature (T_f), the temperature at 5% weight loss ($T_{5\%}$), and the second decomposition temperature (T_s) are summarized in Table II. It was clear that the MeHHPA-cured SiE resins had a higher thermal stability than the MeHHPA-cured CEL-2021P.

SiE-2 showed the highest $T_{5\%}$ and T_f values; this implied that the SiE resin with the moderate epoxy value had the highest thermal stability. This was because the thermal stability of the SiE resins increased with increasing silicon content and increasing crosslinking density; the silicon–epoxy resin with a higher silicon content had a lower

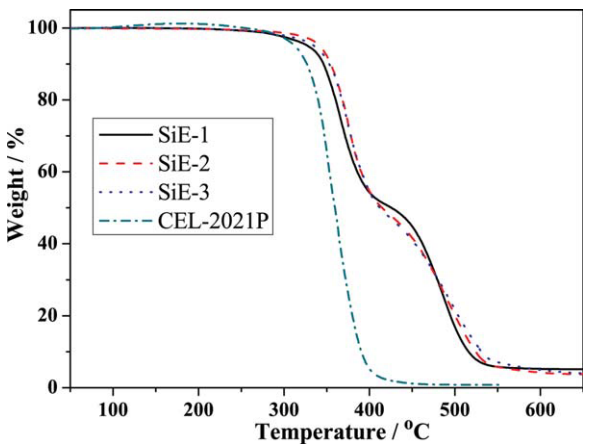

Figure 6 Transmittance spectra of the MeHHPA-cured SiE resins and CEL-2021P. [Color figure can be viewed in the online issue, which is available at wileyonlinelibrary.com.]

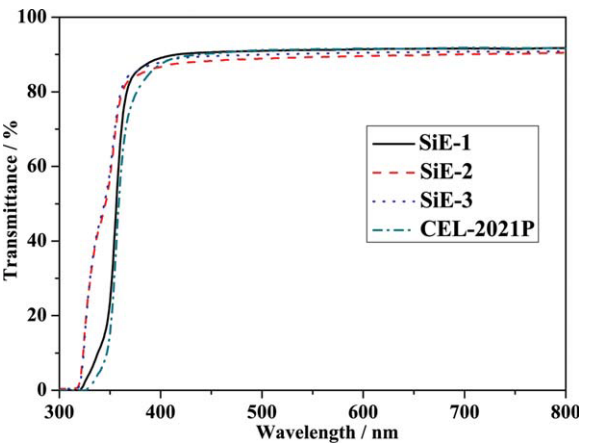

Figure 7 TGA thermograms of the MeHHPA-cured SiE resins and CEL-2021P. [Color figure can be viewed in the online issue, which is available at wileyonlinelibrary.com.]

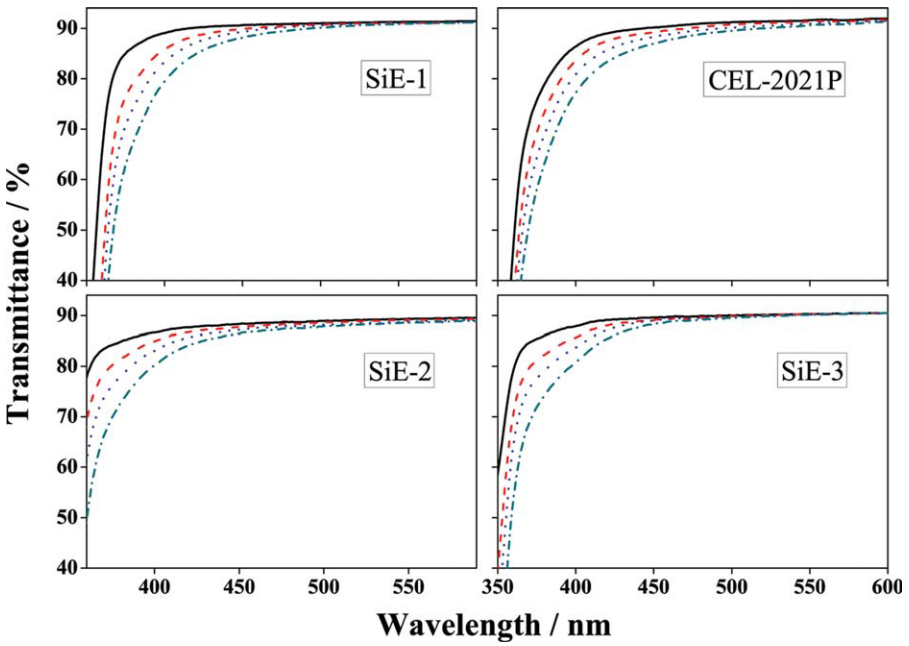

Figure 8 Transmittance spectra of the MeHHPA-cured SiE resins and CEL-2021P during thermal aging: (—) before aging, (- - -) after 72 h of aging, (· · ·) after 144 h of aging, and (-·-) after 260 h of aging. [Color figure can be viewed in the online issue, which is available at wileyonlinelibrary.com.]

epoxy value, and consequently, the cure resin had a lower crosslinking density, with the assumption that the curing reaction for all of the resins was complete. Thus, the highest thermal stability was achieved at a compromise between the silicon content and the epoxy value.

Thermal and UV aging performances of the cured resins

The thermal and UV aging performances of the cured materials were characterized by the changes in transmittance over the range 300–800 nm after aging, as shown in Figures 8 and 9, respectively. At

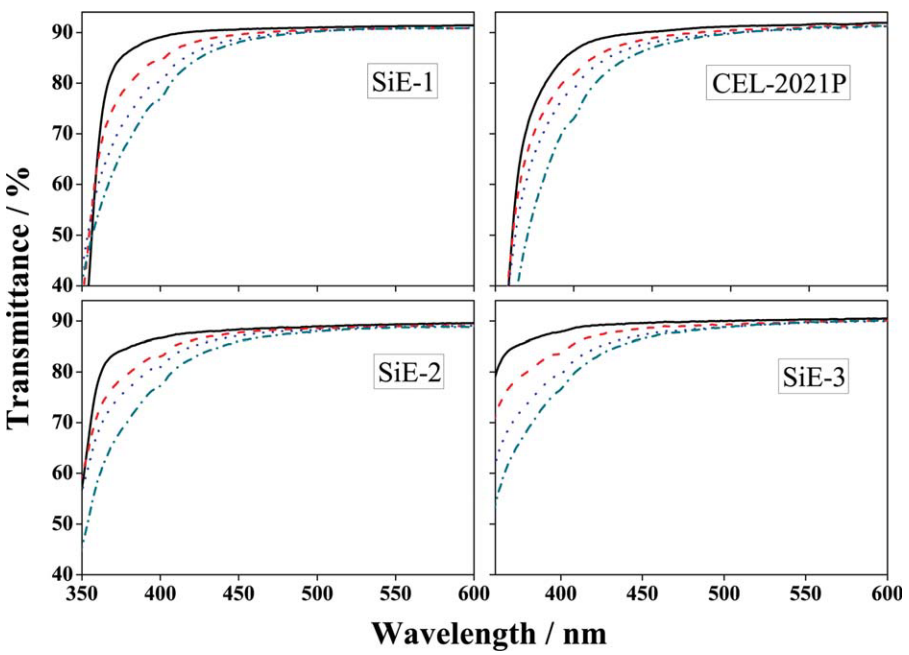

Figure 9 Transmittance spectra of the MeHHPA-cured SiE resins and CEL-2021P during UV aging: (—) before aging, (- - -) after 24 h of aging, (· · ·) after 72 h of aging, and (-·-) after 192 h of aging. [Color figure can be viewed in the online issue, which is available at wileyonlinelibrary.com.]

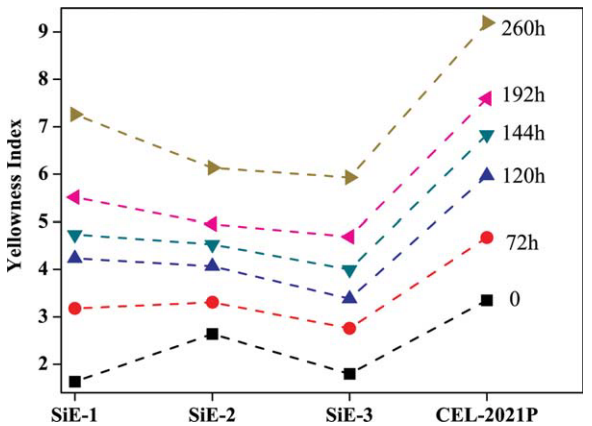

Figure 10 Change in YI over time for the MeHHPA-cured SiE resins and CEL-2021P during thermal aging. [Color figure can be viewed in the online issue, which is available at wileyonlinelibrary.com.]

any stage of UV or thermal aging, CEL-2021P showed a lower transmittance than the SiE resins in the purple region (455–390 nm), which meant it absorbed more purple light and displayed more yellowing.

On the basis of the transmittance spectra, YI of the cured materials was calculated with the following equation:[19]

$$YI = 100 \times (T_{680} - T_{420})/T_{560}$$

where T_{680}, T_{420}, and T_{560} are the transmittances of the samples at 680, 420, and 560 nm, respectively. The degree of discoloration was characterized by the increase in YI during thermal and UV aging (Figs. 10 and 11).

For both thermal and UV aging, the SiE-2 resin showed the best resistance to discoloration, and CEL-2021P exhibited the most serious discoloration. Morita et al.[7] reported that the thermal aging resistance of SiE resins was proportional to the silicon content. Here, we considered that the aging performance of the SiE resins, just like thermal stability, was influenced not only by the silicon content but also by the crosslinking density. As a result, the highest thermal and UV resistances were obtained by a compromise between the silicon content and the epoxy value, as discussed previously.

TABLE III
Atomic Si/C Ratios for the Cured SiE Resins

Si/C		
Bulk[a]	Surface[b]	Surface/bulk ratio
0.128	0.171	1.34
0.190	0.283	1.49
0.235	0.481	2.05

[a] Calculated with the formulations of the cured resins.
[b] Determined from X-ray photoelectron spectroscopy measurements.

Comparing the aging performance of SiE-1 with SiE-3, we observed that the former showed better resistance to UV aging, whereas the latter showed better resistance to thermal aging. This may have been due to the surface enrichment of siloxane because of its low surface energy. The surface enrichment of siloxane for the epoxy resins was characterized with the atomic ratio of silicon to carbon (Si/C) of the surface layer (as measured by X-ray photoelectron spectroscopy) and compared to that of the bulk (Table III). It was likely that the thermal oxidation of the surface of the cured resins was more serious than that of the bulk during thermal aging, and the enriched siloxane acted as a protecting layer against thermal oxidation. The enrichment degree of siloxane was enhanced with increasing silicon content (or decreasing epoxy value), as shown in Table III; thus,

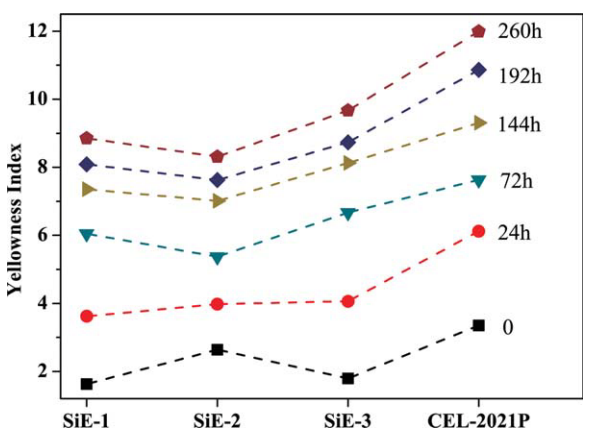

Figure 11 Change in YI over time for the MeHHPA-cured SiE resins and CEL-2021P during UV aging. [Color figure can be viewed in the online issue, which is available at wileyonlinelibrary.com.]

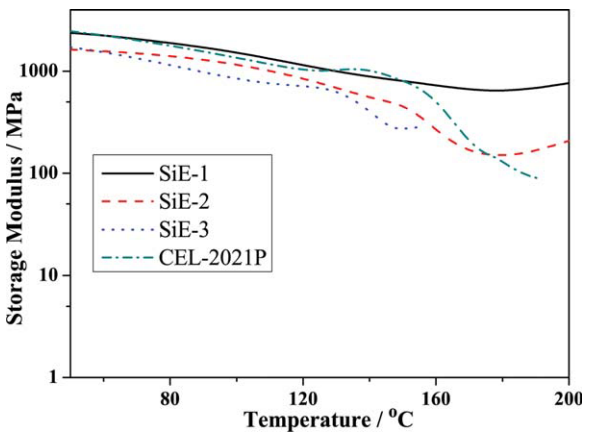

Figure 12 Storage modulus versus the temperature for the MeHHPA-cured SiE resins and CEL-2021P. [Color figure can be viewed in the online issue, which is available at wileyonlinelibrary.com.]

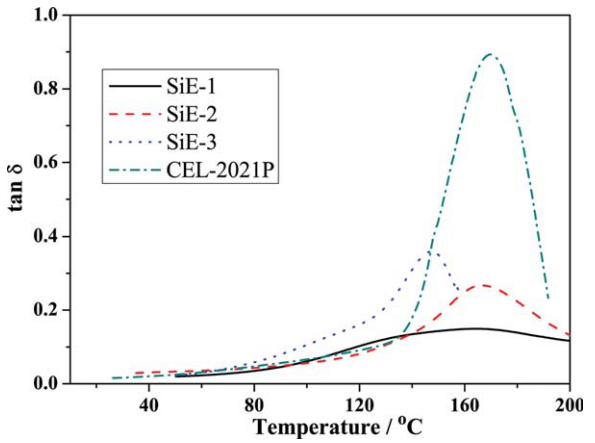

Figure 13 Tan δ versus the temperature for the MeHHPA-cured SiE resins and CEL-2021P. [Color figure can be viewed in the online issue, which is available at wileyonlinelibrary.com.]

the silicon content played a more important role than the crosslinking density for thermal aging.

However, the surface enrichment of siloxane was not so effective for the improvement of the UV resistance. This was reasonable because surface oxidation was not pronounced in this case. Therefore, the crosslinking density of the resins played a more important role than the silicon content, and SiE-3 showed poorer UV resistance than did SiE-1.

In the CEL-2021P resin, an antioxidant and a UV stabilizer were added, whereas no additives were used for the SiE resins in this study. We believe that the thermal and UV aging performances could be further improved by the introduction of some specific antioxidants and UV stabilizers.

Mechanical properties

The mechanical properties of the cured SiE resins were determined with DMA, TMA, and hardness measurements. The storage modulus and loss factor (tan δ), measured by DMA, are shown in Figures 12 and 13, respectively. The glass-transition temperature (T_g) was determined as the peak temperature of the tan δ curve (Table IV). The mechanical properties were greatly affected by the crosslinking density, which was directly related to the epoxy value. The cured SiE-1 showed a wide and flat tan δ peak; thus, it was difficult to determine its T_g; actually, it did not exhibit an obvious decrease in the storage modulus during the scanning range. This indicated that the cured SiE-1 was very rigid because of a very high crosslinking density. With decreasing epoxy value, SiE resins became flexible, and the storage modulus and T_g decreased.

In general, the height of the α-transition peak [$(\tan \delta)_{max}$] for thermosetting resins is related to the mobility of the polymer chain segments; a higher $(\tan \delta)_{max}$ means a longer distance between crosslinks. As shown in Figure 13, the order of $(\tan \delta)_{max}$ for SiE was as follows: SiE-3 > SiE-2 > SiE-1; this indicates that a lower epoxy value resulted in a less densely crosslinked network and a higher mobility of chain segments. This was consistent with the analysis of the storage modulus and T_g. Of course, the crosslinking density was related not only to the epoxy value but also to the functionality of resin. This is why CEL-2021P showed the highest $(\tan \delta)_{max}$, although it had the highest epoxy value of 0.74; it was a two-functional epoxy resin, whereas the SiE resins were multifunctional.

It was reported that the full width at half-maximum of the α relaxation peak was sensitive to the homogeneity of the networks.[18] In this case, as the epoxy value increased, the tan δ peak became broader and covered a wider temperature range; this indicated a more nonuniform distribution of chain lengths between crosslinks. SiE-1 showed the largest full width at half-maximum of the α relaxation peak, mainly because it had the most side epoxy groups bonded to siloxane main chains among the SiE resins. The curing reaction of the SiE resin with anhydride was a random process, which occurred at either the interchain or intrachain; SiE-1 was inclined to form the most complicated network with the widest distribution of chain lengths between crosslinking sites.

Table IV also gives the TMA and hardness results. The coefficients of linear thermal expansion of the SiE resins below T_g (α_1) and above T_g (α_2) both

TABLE IV
Mechanical Properties of the MeHHPA-Cured SiE Resins and CEL-2021P

Resin	Storage modulus at 50°C (Pa)	T_g (°C)	CTE (ppm) α_1	CTE (ppm) α_2	Hardness (Shore D)
SiE-1	2.39×10^9	—	66.51	101.3	91
SiE-2	1.63×10^9	166.6	76.03	159.8	88
SiE-3	1.73×10^9	147.5	94.43	180.5	86
CEL-2021P	2.47×10^9	169.7	53.49	80.49	91

CTE = coefficient of thermal expansion.

increased with increasing silicon content. All three silcone–epoxy resins showed larger coefficients compared to CEL-2021P. This implied that the coefficients of linear thermal expansion depended not only on the density of polymer network but also on the flexibility of the molecular chains. Hardness measurements showed that SiE-1 was as hard as CEL-2021P, and SiE-2 and SiE-3 were a bit softer. These results confirmed, again, that the SiE resins became more flexible with decreasing epoxy value.

CONCLUSIONS

SiE resins with different epoxy values were synthesized through the base-catalyzed hydrolytic condensation of EMDS and the cohydrolytic condensation of EMDS with dimethyldiethoxysilane. These resins were linear oligomers bearing pendant epoxy groups; the average number of repeat Si—O units ranged from 6 to 11. The structures of the SiE resins were confirmed by ^{1}H-NMR, ^{29}Si-NMR, and MALDI-TOF–MS spectra. MeHHPA was used to cure the SiE resins; they showed a similar curing reactivity to the epoxy resin CEL-2021P, and the cured resins exhibited a high optical clarity. The SiE resins were superior to CEL-2021P in thermal stability and thermal and UV resistances. SiE-2 displayed the highest thermal and UV resistances because it had an optimal balance between the silicon content and crosslinking density. DMA, TMA, and hardness analysis showed that a decrease in the epoxy value made the SiE resins more flexible. Because of the adjustable viscosity, good thermal and mechanical properties, and high thermal and UV resistances, the SiE resins are very promising materials for LED packaging.

References

1. Huang, J.-C.; Chu, Y.-P.; Wei, M.; Deanin, R. D. Adv Polym Technol 2004, 23, 298.
2. Maehara, T.; Takenaka, J.; Tanaka, K.; Yamaguchi, M.; Yamamoto, H.; Ohshita, J. J Appl Polym Sci 2009, 112, 496.
3. Yoshikawa, Y. U.S. Pat. 2008124822-A1 (2008).
4. Huang, W.; Zhang, Y.; Yu, Y.; Yuan, Y. J Appl Polym Sci 2007, 104, 3954.
5. Kashiwagi, T.; Shiobara, T. U.S. Pat. 2005244649-A1 (2005).
6. Morita, Y. J Appl Polym Sci 2005, 97, 946.
7. Morita, Y.; Tajima, S.; Suzuki, H.; Sugino, H. J Appl Polym Sci 2006, 100, 2010.
8. Morita, Y.; Tajima, S.; Suzuki, H.; Sugino, H. J Appl Polym Sci 2008, 109, 1808.
9. Morita, Y. J Appl Polym Sci 2009, 114, 2301.
10. Imazawa, K.; Kashiwagi, T.; Kojima, T.; Shiobara, T. U.S. Pat. 2006270808-A1 (2007).
11. Crivello, J. V.; Bi, D. J Polym Sci Part A: Polym Chem 1993, 31, 3121.
12. Crivello, J. V.; Lee, J. L. J Polym Sci Part A: Polym Chem 1990, 28, 479.
13. Crivello, J. V.; Mao, Z. B. Chem Mater 1997, 9, 1554.
14. Crivello, J. V.; Song, K. Y.; Choshal, R. Chem Mater 2001, 13, 1932.
15. Hase, S.; Kobayashi, K. Jpn. Pat. 2008248170-A (2008).
16. Kobayashi, H.; Hirai, N.; Okawa, K. Jpn. Pat. 2008120843-A (2008).
17. Morita, Y.; Sugino, H. J Appl Polym Sci 2006, 100, 962.
18. Hou, S. S.; Chung, Y. P.; Chan, C. K.; Kuo, P. L. Polymer 2000, 41, 3263.
19. Billmeye, F. W. Mater Res Stand 1966, 6, 295.